Advances in Colloid and Interface Science 164 (2011) 12–20

Contents lists available at ScienceDirect

Advances in Colloid and Interface Science

journal homepage: www.elsevier.com/locate/cis

Positively charged nanofiltration membranes: Review of current fabrication methods and introduction of a novel approach

Shuying Cheng, Darren L. Oatley, Paul M. Williams, Chris J. Wright *

Centre for Complex Fluids Processing, Multidisciplinary Nanotechnology Centre, School of Engineering, Swansea University, Singleton Park, Swansea SA2 8PP, UK

ARTICLE INFO

Available online 20 January 2011

Keywords:
Nanofiltration
Positive charge
Surface modification
Atomic force microscopy

ABSTRACT

A review of the fabrication processes currently available to produce positively charged nanofiltration membranes has been conducted. The review highlights that there are few membranes and studies currently available. The preparation of a novel positively charged nanofiltration membrane is also described. This membrane was fabricated by surface modification of a prepared base membrane using polyethyleneimine followed by cross linking with butanedioldiglycidylether. The fabrication process uses standard organic solvents and avoids the need for hazardous materials, such as concentrated sulphuric acid, which significantly benefits the scale up potential of any future commercial manufacturing process.

The new membrane was characterised using a number of state-of-the-art techniques, including a novel use of atomic force microscopy to determine pore size. Streaming potential measurements confirmed that this new membrane is indeed positively charged in the pH range below pH 9, which covers the majority of normal operating conditions. The performance characteristics for the new membrane were very favourable, with a pure water flux determined to be 20 LMH bar^{-1} and a rejection of MgCl of 96%. Thus, this new membrane both adds to and complements the existing short supply of positively charged NF membranes and is suitable for applications such as the recovery of valuable cationic macromolecules in the bioprocess and pharmaceutical industries or removal of multi-valent cations such as dyes and heavy metals in the paper and pulp, textiles, nuclear, and automotive industries.

Contents

* Corresponding author. Tel.: +44 1792 295 200.
E-mail address: C.Wright@swansea.ac.uk (C.J. Wright).

0001-8686/$ – see front matter © 2011 Elsevier B.V. All rights reserved.
doi:10.1016/j.cis.2010.12.010

1. Introduction

Nanofiltration (NF) is a pressure driven membrane separation process with characteristics between reverse osmosis and ultrafiltration. The nominal molecular weight cut off of a NF membrane is in the range 100–1000 Da, indicating that NF membranes have an approximate pore size of 1 nm. Separation of solutes in the NF range is dependent upon the micro-hydrodynamics and interfacial events occurring at the membrane surface and inside the membrane pore. Rejection may be attributed to a combination of both steric and charge effects.

Nanofiltration was introduced in the early 1980s and has since gained in popularity due to improved selectivity for mono and multi valent ions, low operating pressures and relatively low capital and operating costs. To date, as a direct result of the fabrication materials traditionally employed, most NF membranes are either neutral or negatively charged in an aqueous processing environment. These polymeric membranes are often amphoteric in nature and can exhibit a net positive charge at low pH, typically less than pH 4 [1,2]. This has led to some confusion over the actual charge nature of some negatively charged membranes and is the result of much confusion between membrane manufacturers, end users and the literature [3]. Positively charged NF membranes can have excellent hydrophilicity and exhibit high rejections for multi valent cations. These properties are particularly important for recovery of valuable cationic macromolecules in the bioprocess and pharmaceutical industries or removal of multi valent cations such as dyes and heavy metals from effluents in the paper and pulp, textiles, nuclear, and automotive industries. The distinct lack of positively charged NF membranes is true of both the commercial and laboratory environment alike and very limited studies are currently available that utilize positively charged NF membranes.

Du and Zhao [4,5] were the first to produce a positively charged NF membrane using poly(N,N-dimethylaminoethyl methacrylate). The poly(N,N-dimethylaminoethyl methacrylate) was first purified by ultrafiltration and then cast as an aqueous solution onto a polysulfone microfilter that acted as a mechanical support plate. Following slight drying, the new membrane was cross linked by immersion in p-xylylene dichloride/heptane solution. The resulting NF membrane exhibited a best rejection of 90% for $MgSO_4$, with a membrane flux of 10–20 LMH at 8 bar. Wang and co-workers [6] investigated the effects of pH and $NaHCO_3$ concentration in the casting solution of a similar membrane. They determined that a uniform top layer is obtained through stabilising the pH of the casting solution during the pre-drying phase of the fabrication process. Stabilisation at different pH values had a profound impact on the membrane separation properties with a maximum NaCl rejection (93%) and flux (24 LMH at 8 bar) at pH 7. The relationship between rejection and flux was counter intuitive, i.e. one would normally expect lower rejection at high flux, and the workers acknowledged this fact but had no explanation. A similar effect was noted when varying the salt concentration added to the casting solution, producing a maximum rejection for $MgSO_4$ of 91% (no flux data was provided). This value is similar to the performance of the membrane produced by Du and Zhao [4,5] described previously. Huang et al. [7] produced a positive NF membrane using a copolymer graft of trimethylallyl ammonium chloride onto chitosan as the active top layer. Quaternation was applied to modify the chitosan in order to improve hydrophilicity and introduce the positively charged groups. This solution was cast onto a polyacrylonitrile ultrafiltration membrane as the support and then cross linked with toluene diisocyante. The molecular weight cut off of the resulting membrane was determined to be 930 Da and the membrane performance was reasonable, with a rejection of $MgCl_2$ greater than 90% in some cases and a modest membrane flux of 8.5 LMH at 12 bar. In an analogous study, the same workers [8] produced a membrane by substituting trimethylallyl ammonium chloride for 2-hydroxypropyltrimethyl ammonium chloride. This membrane exhibited a reduced molecular weight cut off of 560 Da, a rejection of $MgCl_2$ approaching 97%, and an improved membrane flux of 14–18 LMH at 12 bar. Tongwen and Weihua [9] prepared a new membrane using 2,6-dimethyl-1,4-phenylene oxide dissolved in chlorobenzene and then brominated, the resulting solution was precipitated by addition of methanol and dried to form the primary membrane polymer. This brominated primary polymer was dissolved in chloroform and cast onto a substrate membrane (prepared from similar materials) and then cross linked *in situ* using a mixture of trimethylamine and ethylenediamine. The resulting membrane best case performance achieved a very favourable flux (63 LMH at 2.5 bar) but exhibited a low rejection value of 73% for $MgCl_2$. Each of the membranes described above was prepared by interfacial polymerisation upon a substrate micro or ultra filter to produce a composite NF membrane. The production of composite membranes is generally considered to be complex. Each of the fabrication processes described above uses hazardous or carcinogenic materials, involves several preparation stages, is time consuming, and offers little potential to be expanded to an economical full scale production process. Integrally skinned asymmetric membranes offer a direct alternative and are fabricated using the more simplistic phase inversion technique [10].

Tang et al. [11–13] produced a membrane using the same materials as Tongwen and Weihua [9]. In this case, the membrane was formed by phase inversion using an ethanol bath rather than cast onto a substrate membrane. The authors studied the influence of several fabrication parameters on the membrane performance and morphology. However, characterisation of the resulting membrane demonstrated a best pore size distribution in the range 7 to 10 nm which is in the ultrafiltration range. Su et al. [14] produced an asymmetric base membrane using the phase inversion technique from chloromethylated poly(phthalazinone ether sulfone ketone) dissolved in N-methyl-2-pyrrolidine and cast onto glass sheets at 60 °C prior to immersion in water. The base membrane was then immersed into a solution containing trimethylamine to induct quaternary nitrogen groups into the membrane. Thus, applying a surface modification to the original asymmetric membrane and introducing a positively charged quaternized surface layer. The effects of evaporation time, coagulation temperature and additives in the fabrication bath were studied and membrane performance was optimised. The resulting membranes exhibited excellent pure water flux performance, around 154 LMH at 2 bar, whilst maintaining almost 100% rejection of the dyes Clayton Yellow (MW = 696 Da) and Methyl Orange (MW = 327 Da). The rejection of $MgCl_2$ for this same membrane was low at a value of 20%. Interestingly, when a series of rejection experiments using different dyes were conducted for this membrane, the rejections of dyes X-6G, X-8B and Methyl Orange (all negatively charged) were all higher than the rejections of dyes Methylene Blue, Centian Violet and Malachite Green (all positively charged). The authors explain this phenomenon by assuming that the increased rejection of the negative dyes are the result of steric partitioning caused by increased aggregation of these dye species and not the result of Donnan effects. If this were to be the case, then the fact that the new membrane is positively charged has no bearing on this specific separation. In addition, the possibility arises that this membrane could in fact exhibit a net negative charge as there is no direct evidence presented confirming that this membrane is indeed positively charged (i.e. via streaming potential measurement or equivalent) and the positive nature of this membrane is only assumed as a result of the quaternization procedure. Yan and co-workers [15,16] produced an NF membrane using similar methods and materials as Su et al. [14]. Poly(phthalazinone ether sulfone ketone) was dissolved in concentrated sulphuric acid and reacted with chloromethyl octyl ether to form the base membrane material which was prepared by phase inversion. The base membrane was then soaked in trimethylamine solution to allow chemical adsorption

and self assembly formation of the positively charged membrane. The resultant membrane exhibited similar performance as those previous [4–8], with a $MgCl_2$ rejection of 84% and a membrane flux of 49 LMH at 4 bar. The observation was also made that the membrane flux could be significantly improved by increasing the processing temperature (from 30 LMH at 15 °C to 120 LMH at 85 °C) with little detriment to the rejection performance (82% to 75% respectively). As for Su et al. [14], Yan and co-workers [15,16] failed to directly measure the membrane charge properties. However, the rejection characteristics for a series of salts were provided, where $R(MgCl_2)>R(MgSO_4)>R(NaCl)>R(Na_2SO_4)$, inferring that the membrane formed was indeed positively charged.

In the following sections of this paper, the fabrication of a novel positively charged NF membrane using the phase inversion technique followed by chemical adsorption is demonstrated, although avoiding the need to use hazardous materials such as concentrated sulphuric acid in the production process. Furthermore, the influence of fabrication conditions in order to produce a membrane of superior processing performance is investigated. The modified membrane is also characterised using an array of state-of-the-art techniques, including a novel use of atomic force microscopy (AFM), in order to clearly demonstrate both the physical properties and separation performance.

2. Experimental

2.1. Substrate membrane formation

The membranes fabricated and characterised in this study were prepared in the Swansea laboratory. A flat sheet polyetherimide/sulfonated polyether ether ketone blend membrane (A6DT) was made using the traditional phase inversion method from a N-methylpyrrolidone (NMP)/tetrahydrofuran (THF)/dioxane solution of the polymers using a doctor blade (CAMAG), described previously [17].

2.2. Surface modification

The negatively charged A6DT blend membranes were immersed in an aqueous solution of 5 g l^{-1} polyethyleneimine (pH 10.5, which is the original pH value of the polyethyleneimine solution) for 8 h. Polyethyleneimine was deposited on the substrate membrane via electrostatic interactions, to fabricate a new positively charged membrane PA6DT. The modified membranes were washed with deionised (DI) water three times and then stored in DI water. Polyethylenimine (50% in water) and butanedioldiglycidylether (BUDGE) were purchased from Sigma-Aldrich, UK. Polyethyleneimine is a water-soluble polymer. In order to improve the stability of the PA6DT modified membranes, BUDGE was used as a cross-linking agent on the membrane surface [18]. The modified membranes were immersed in 50 ml of a 5% (V/V) BUDGE in methanol solution and allowed to react overnight to obtain a cross-linked positive membrane. The reaction of cross-linking is shown in Fig. 1. The membranes were then washed with methanol and DI water three times respectively. The cross-linked modified membrane was denoted as PA6DT-C and was stored in DI water until characterisation.

Membrane modification at lower pH values was also completed to obtain other types of modified membrane, using 0.1 M HCl to change the pH value of polyethyleneimine solution from pH 10.5 to pH 8 and pH 6. The substrate membrane was placed in a mixed solution of 5 g l^{-1} polyethyleneimine and 100.0 mol m^{-3} NaCl, which was then used to study the effect of salt in the casting solution on the characteristics of the resulting membrane. The modification conditions are provided in Table 1.

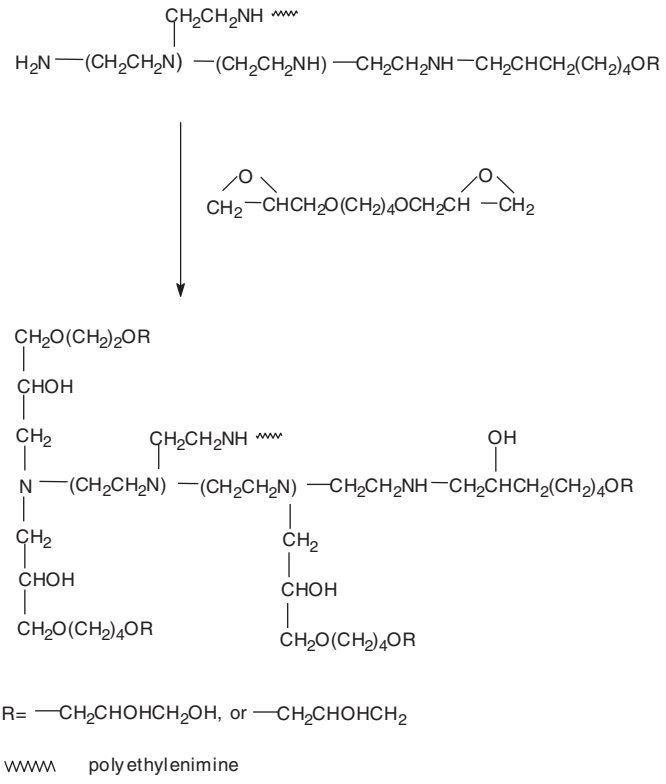

Fig. 1. Cross-link reaction for polyethylenimine with BUDGE.

2.3. Membrane characterisation

2.3.1. Zeta potential measurement

The zeta potential (ζ-potential) was determined with an electrokinetic analyser (EKA, Anton Paar KG, Graz, Austria) based on the streaming potential method [2,3]. Flat sheets of the membranes were used as samples to study the influence of pH of the solution on the membrane ζ-potential. The streaming potential was measured by forcing the electrolyte solutions through a thin slit channel ($90\times10\times0.27$ mm) formed by a PVTF spacer between two membranes facing each other, for continuously increasing values of pressure (up to 200–240 mbar). The ζ-potential was calculated using the Smoluchowski equation. The pH and conductivity of the solutions were also measured. The ζ-potential was measured in 1.0 mol m^{-3} KCl over a pH range of 3.5 to 11.0, altered by addition of 0.1 M HCl or 0.1 M NaOH, at 25 ± 0.5 °C.

2.3.2. Frontal filtration experiments

Frontal filtration was used to measure the water permeability and rejection of the modified membranes using constant feed conditions over a range of pressures, as described in previous studies [17]. All experiments were conducted at room temperature (20 ± 2 °C) and a

Table 1
Modification conditions for membrane A6DT.

Membrane	pH	NaCl (mol m^{-3})
PA6DT-C (6)	6	–
PA6DT-C (8)	8	–
PA6DT-C	10.5	–
PA6DT-S-C	10.5	100

P - the polyethyleneimine modified membrane,
C - membrane cross-linking, and
S - the addition of salt in the modification solution.
The numbers represent pH values of the modification solution.

pH of 5.8–6.0 (which is the pH of the pure water used in the study), except when indicated otherwise. All filtration experiments were carried out in an Amicon 8050 cell with 50 ml of fresh feed solution and an effective membrane area of 13.4×10^{-4} m^2. The water permeability of each membrane was measured in a pressure range of 100 and 500 kPa. Solute rejection was measured using 0.1 g l^{-1} Vitamin B12, 0.1 g l^{-1} PEG 1500, and 1.0 mol m^{-3} salts (NaCl, Na_2SO_4, $MgCl_2$ and $MgSO_4$) over the same pressure range. Vitamin B12 (MW = 1355 Da) and PEG1500 were supplied by Sigma-Aldrich, UK. All the salts were supplied by Fisher-Scientific UK. Rejection was based on measurement of 15 ml of permeate after the first 4 ml permeate was discarded. The membrane was washed with DI water after each experimental run to thoroughly remove the remains of the previous solute. Data from filtration experiments was used to calculate the water permeability and effective pore radius; this method has been extensively discussed in previous work [17,19,20]. These parameters were used to compare the process performance of the unmodified and modified membranes. Rejection of solute was calculated using the following equation,

$$R_{obs} = 1-\frac{C_p}{C_b} \tag{1}$$

where C_p and C_b are the concentration of permeate solution and feed solution respectively. As a result of concentration polarization, the concentration of a solute at the membrane wall is higher than that of the bulk. Therefore, real rejection is defined as,

$$R_{real} = 1-\frac{C_p}{C_w} \tag{2}$$

where C_w is the solute concentration at the membrane surface. The value of C_w may be calculated indirectly from the bulk feed solute concentration (C_b) using a mass transfer correlation [21]. As the sample size is significant in comparison to the total volume of the Amicon 8050 cell, the feed concentration was taken as the average from the start and end of the experiment, i.e.

$$C_b = \frac{1}{2}\left(C_{b,start} + C_{b,end}\right). \tag{3}$$

Membrane flux (F) was calculated as

$$F = \frac{W}{At} \tag{4}$$

where W is the mass of pure water or solution permeated during the experiment, A is the membrane area and t is the experimental time.

2.3.3. Atomic force microscopy — membrane structural characterisation and topography

AFM of the membrane surface was conducted using a Dimension 3100 AFM (Veeco Instruments, Santa Barbara, CA) in tapping mode to image (in air) the surface topography by probing the surface with an oscillating tip. Standard tapping mode cantilevers (Olympus, Japan) with a spring constant of 42 N/m and a typical tip apex of 5 nm were used. Phase images captured simultaneously with topographic images were used to study the properties of the membrane. Phase imaging is the mapping of the phase lag between the periodic signal that drives the cantilever and the oscillations of the cantilever [22]. Using tapping mode AFM, the phase shift is derived from the difference in phase angle between the freely oscillating cantilever in air and the cantilever oscillation during scanning. Changes in the phase lag during tapping mode operation often indicate changes in the properties of the sample surface [23,24]. The phase shift is zero when there is no interaction between the tip or the cantilever and the sample surface. The phase signal is collected alongside the tapping mode topography data and represents the phase angle between the applied and the actual vibration of the tapping tip. Thus, the phase signal is a function of the mechanical properties of the material under the tip, the interaction forces, and the area of contact between tip and surface (i.e. any change in topography).

2.3.4. Scanning electron microscopy — membrane cross section analysis

Scanning electron microscopy (SEM) was used to image the cross-section of the asymmetric membranes formed. The membranes were immersed in ethanol followed by cyclohexane for 2 h respectively and then dried in air. The dried membranes were then cryogenically fractured in liquid nitrogen and coated with Pt/Pd. During the preparation of the membrane sample, care was taken to avoid damage or the creation of artefacts in the membrane structure. The instrument used was a Philips XL30 CP SEM (FEI, The Netherlands).

3. Results and discussion

3.1. Zeta potential measurements

Fig. 2 presents the pH dependence of ζ-potential of membrane A6DT and modified membranes PA6DT and PA6DT-C in 1.0 mol m^{-3} KCl. The charge reversal of the new membranes and significant shift in the isoelectric point (IEP) from that of the substrate membrane (A6DT) due to the adsorption of polyethyleneimine followed by BUDGE is clearly observed. The ζ-potential of the membrane A6DT had a near zero value at pH 3.5, which is the IEP of SPEEK. The IEP determined for the new membranes PA6DT and PA6DT-C was at pH values 10.2 and 9.0 respectively. Therefore, at low pH values (below IEP), the new membranes are positively charged and will become negatively charged above the IEP. The IEP of the cross linked membrane PA6DT-C is lower than that of membrane PA6DT as some of the exposed amino groups at the membrane surface have formed ether bonds in the reaction with BUDGE. The shift in the IEP value for the new membranes represents approximately 7 pH units and indicates that both new membranes will be positively charged under the majority of practical processing conditions. Interestingly, the magnitude of the ζ-potential for membrane PA6DT is greater than that of PA6DT-C over the entire range studied, thus indicating that there is a net trade in the magnitude of membrane fixed charge for an improved membrane stability.

3.2. Water permeability

The pure DI water flux was measured for each membrane using an applied pressure range of 100–500 kPa. Water permeability can be determined from the slope of the straight line obtained when plotting the variation of the water flux versus the applied pressure. Table 2

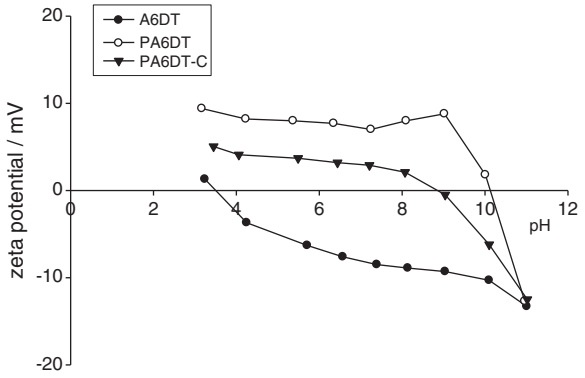

Fig. 2. Zeta potential as a function of pH (background electrolyte 1.0 mol m^{-3} KCl).

Table 2
Characteristics of modified and basic membranes.

Membranes	P_m $m^3s^{-1}N^{-1}\times10^{11}$	R_{real} [a] *PEG1500*	r_p [a] nm	R_{real} [b] *B12*	r_p [b] nm	R_{real} [c] *NaCl*	X_d mol m^{-3}
A6DT	27.5 ± 1.9	0.692	2.07	–	–	0.5790	−45.8
PA6DT-C (6)	16.2 ± 0.02	0.8243	1.74	0.5424	1.65	0.4553	3.8
PA6DT-C (8)	13.6 ± 0.23	0.9151	1.51	0.5790	1.49	0.5937	8.3
PA6DT-C	5.34 ± 0.48	0.9274	1.47	0.6408	1.46	0.8249	12.5
PA6DT-S-C	3.70 ± 1.1	0.9316	1.46	0.6690	1.42	0.8524	13.8

For rejection data. 100 kNm^{-2} for A6DT, and 400 kNm^{-2} for all other membranes.
[a] From rejection of the 0.1 g/l PEG1500 solution.
[b] From rejection of the 0.1 g/l Vitamin B12 solution.
[c] From rejection of the 0.001 M NaCl solution.

summarises the permeability of the original and modified membranes. Note that from this point forward only the cross linked membrane is considered due to the poor stability of polyethyleneimine in water for the PA6DT membrane. As expected, the highest pure water flux was achieved by the original A6DT membrane with a value of ca. 100 LMH bar^{-1}. The deposition of polyethyleneimine on the substrate membrane surface resulted in a remarkable decrease in the water flux due to the formation of a more condensed surface layer. The maximum pure water flux achieved for the other membranes was for membrane PA6DT-C(6) at ca. 59 LMH bar^{-1} and the flux order was PA6DT-C(6)>PA6DT-C(8)>PA6DT-C>PA6DT-S-C. The flux value obtained for the membrane PA6DT, prepared under standard conditions, was ca. 19.4 LMH bar^{-1}. This value is almost twice that achieved by Yan and co-workers [15,16] for their asymmetric membrane and is an order of magnitude greater than the flux values obtained using the composite membranes [4–9].

3.3. Frontal filtration experiments

The neutral solute rejection data is presented in Table 2. Each of the new membranes studied exhibited high rejection of the PEG1500, with rejection greater than 90% in all cases except for membrane PA6DT-C(6), which had a lower rejection of 82%. This indicates that membrane PA6DT-C(6) has a more open pore structure than the other membranes and is confirmed by the increased water permeability observed. The rejection of vitamin B12 follows a similar pattern as that for PEG1500 but with lower rejection values. The neutral solute rejections were then used to calculate the effective pore size for the membranes. Membranes PA6DT-C, PA6DT-C(8), and PA6DT-S-C all had a calculated pore size of ca. 1.5 nm, with the PA6DT-C(6) membrane having a slightly larger pore size of around 1.7 nm. Again, this is consistent with the membrane flux and rejection trends observed for these membranes.

The membrane rejection and flux determined over a range of effective pressures for a solution of NaCl using the new membranes are presented in Fig. 3. The highest membrane flux was obtained for membrane PA6DT-S-C; however, this membrane also exhibited the lowest rejection values. The flux of membrane PA6DT-C(8) was only slightly lower than membrane PA6DT-S-C but the rejection performance was improved, by approximately 20%. Membranes PA6DT-C

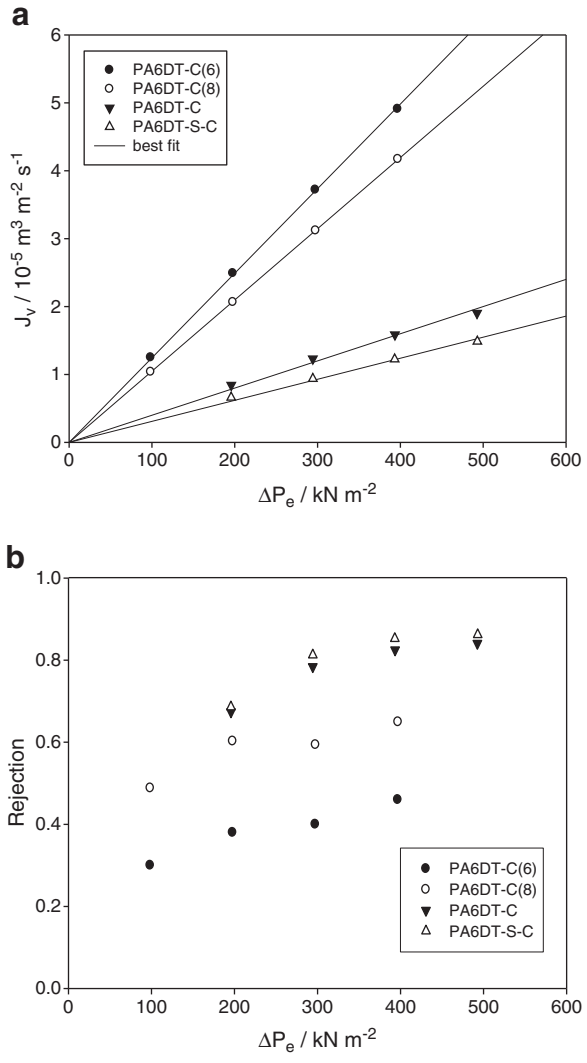

Fig. 3. The effect of effective pressure on the rejection of NaCl solution with concentration of 1 mol m^{-3} at membranes PA6DT-C(6), PA6DT-C(8), PA6DT-C, PA6DT-S-C, and PAA- PA6DT-C. (a) Flux. (b) Rejection.

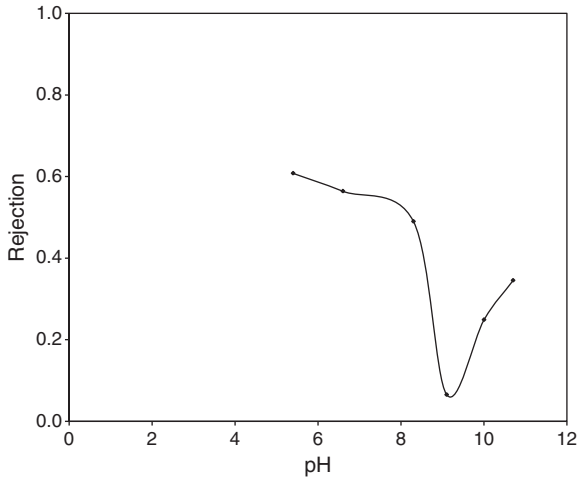

Fig. 4. Determination of the isoelectric point of the modified membrane (PA6DT-C) by rejection of 2.9 mol m^{-3} NaCl.

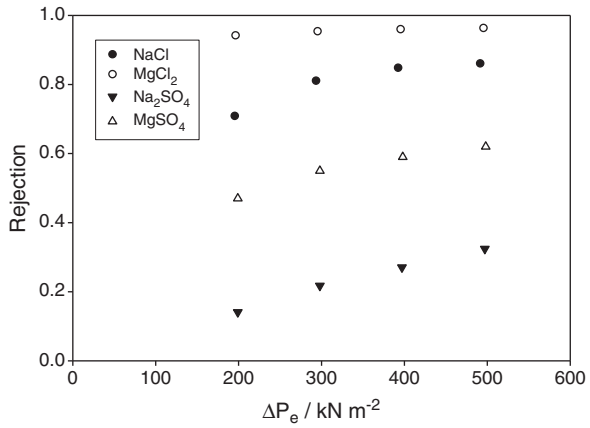

Fig. 5. Salt rejection as a function of effective pressures for membrane PA6DT-C.

and PA6DT-S-C exhibited very similar performance. The flux values obtained for these membranes were significantly lower than those for membranes PA6DT-C(6) and PA6DT-C(8), with the rejection values significantly higher. The NaCl rejection data was also used to calculate the volumetric membrane charge density (X_d), this information is shown in Table 2. The calculated X_d value for membrane PA6DT-C(6) was modest at 3.8 mol m^{-3}, the value for membrane PA6DT-C(8) was double at 8.3 mol m^{-3}, and the values for both membranes PA6DT-C and PA6DT-S-C were triple at 12.5 and 13.8 mol m^{-3} respectively. This indicates that the low rejection and high flux obtained for membrane PA6DT-C(6) are directly attributable to the more open pore size and the lower membrane charge. In comparison, membranes PA6DT-C and PA6DT-S-C both have a higher membrane charge and reduced pore size, which provides explanation of the significantly improved rejection with reduced membrane flux. Membrane PA6DT-C(8) is essentially a compromise between these two extremes, with both a pore size and membrane charge between the values obtained for the other membranes, thus providing explanation for the rejection and flux performance observed. Therefore, a reduction in the solution

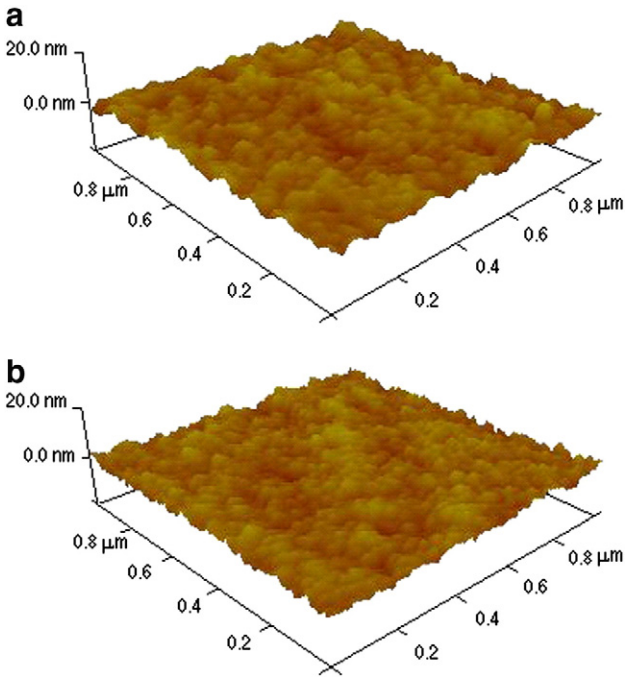

Fig. 6. The three dimensional images of membranes by AFM. (a) A6DT and (b) PA6DT-C.

Table 3
AFM characteristics of the membranes.

AFM characterisation	A6DT	PA6DT-C
r_{AFM} (nm)	4.08 ± 2.64	3.52 ± 1.90
Roughness (nm)	1.39 ± 0.12	1.56 ± 0.10
ε (%)	1.42	0.84

pH during the modification process has the effect of increasing the pore size and reducing the magnitude of charge for the membrane produced. The addition of salt during the modification process has little effect on the properties of the membrane produced as ionic strength does not significantly affect the adsorption of weak polyelectrolytes on a highly charged surface. The slight decrease in membrane flux observed for PA6DT-S-C in comparison to PA6DT-C may be the result of the NaCl screening the electrostatic charges of both polyethyleneimine and the A6DT substrate membrane allowing the formation of a slightly more dense modified surface layer.

The rejection of NaCl from membrane PA6DT-C over a range of pH is presented in Fig. 4. The data clearly indicates a minimum rejection at pH 9 and confirms the isoelectric point previously evaluated from streaming potential measurements. Rejection experiments for membrane PA6DT-C using various single salt solutions were conducted over a range of pressures from 200 kPa to 500 kPa and the results are detailed in Fig. 5. The salt rejection order from high to low is $MgCl_2$>NaCl>$MgSO_4$>Na_2SO_4 and is as expected for a positively

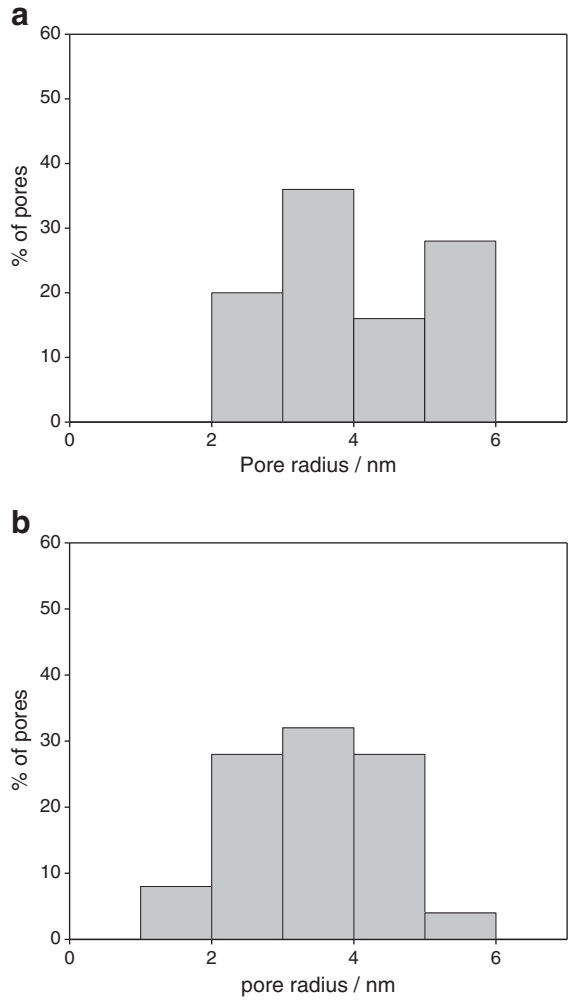

Fig. 7. Pore size distribution for (a) A6DT and (b) PA6DT-C by AFM.

charged membrane. The limiting rejection of $MgCl_2$ was R = 96%. The salt concentration used in this study was less than that used in other published works [15,16], thus a meaningful comparison is not available (this will be addressed in a future study). Nonetheless, a rejection of 96% is considerable. A pore size of 1.47 nm for this membrane indicates that the steric contribution to overall rejection will be very low and the single salt rejections will be dominated by Donnan exclusion [25]. The Donnan exclusion mechanism dictates that a high valence co-ion would be more highly rejected than mono valent co-ion, thus explaining why $MgCl_2$ rejection is higher than NaCl. Also, a high valence counter-ion will actively permeate due to electrostatic attraction, thus explaining why the sulphate salts have lower rejection than the chloride salts, with the magnesium salt being more highly rejected for the previously explained reason.

3.4. Microscopy

AFM topographic images of the substrate membrane (A6DT) and new membrane (PA6DT-C) are presented in Fig. 6. The AFM image analysis program was used to measure surface pore size. Pore sizes were measured by visually inspecting line profiles of different pores. The pore size, roughness and porosity of the substrate membrane and the modified membrane, as measured using AFM, are summarised in Table 3. The average pore size of the A6DT membrane is 4.08 nm. After the deposition of polyethyleneimine and cross linking, the average pore size of PA6DT-C decreased to 3.52 nm. The porosity also decreased with deposition of polyelelctrolyte layers, from 1.42% for A6DT to 0.84% for PA6DT-C. Note that PA6DT-C was made by depositing a thin layer of polyethyleneimine on the A6DT membrane and the hypothesis is made that the reduction in pore size and porosity of the PA6DT-C membrane was a direct result of the deposition of polyethyleneimine layers on the membrane surface and potentially within the pore walls.

Pore size and distribution were quantitatively determined by analysis of the images in conjunction with digitally stored line profiles and are reported in Fig. 7. The modified membrane exhibited relatively narrow pore size distributions. The mean pore size values obtained by the AFM technique were found to be 2.0–2.5 times larger than those calculated from the solute transport data (Table 2). AFM has been employed to measure the pore size of NF filtration membranes previously [26–28]; however, the technique tends to provide a larger pore size than that determined from experimental data due to the limit of AFM resolution. Singh et al. [28] and Bessières et al. [29] also observed that AFM gave 2–4 times larger pore diameters than those obtained from solute transport. Bessières et al. [29] postulated that the pore sizes obtained from solute rejection correspond to a minimal size of the pore constriction experienced by the solute while passing through the pore, whereas pore sizes measured by AFM correspond to the pore entrances on the membrane surface. In the present study pore size was measured at the half way point, as the AFM line trace descended into the pore. A great deal of care must be taken when interpreting images of NF membranes, as the size of the pores are at the limits of the microscopic technique. In Table 3, the pore radius of A6DT was 4.08 nm, but was previously determined to be 1.19 nm [17]. The previous AFM work used an older AFM (Auto probe) in contact mode in contrast to the work presented in this paper which used a state of the art instrument (Dimension 3100) in tapping mode. Comparison between pore size measurements

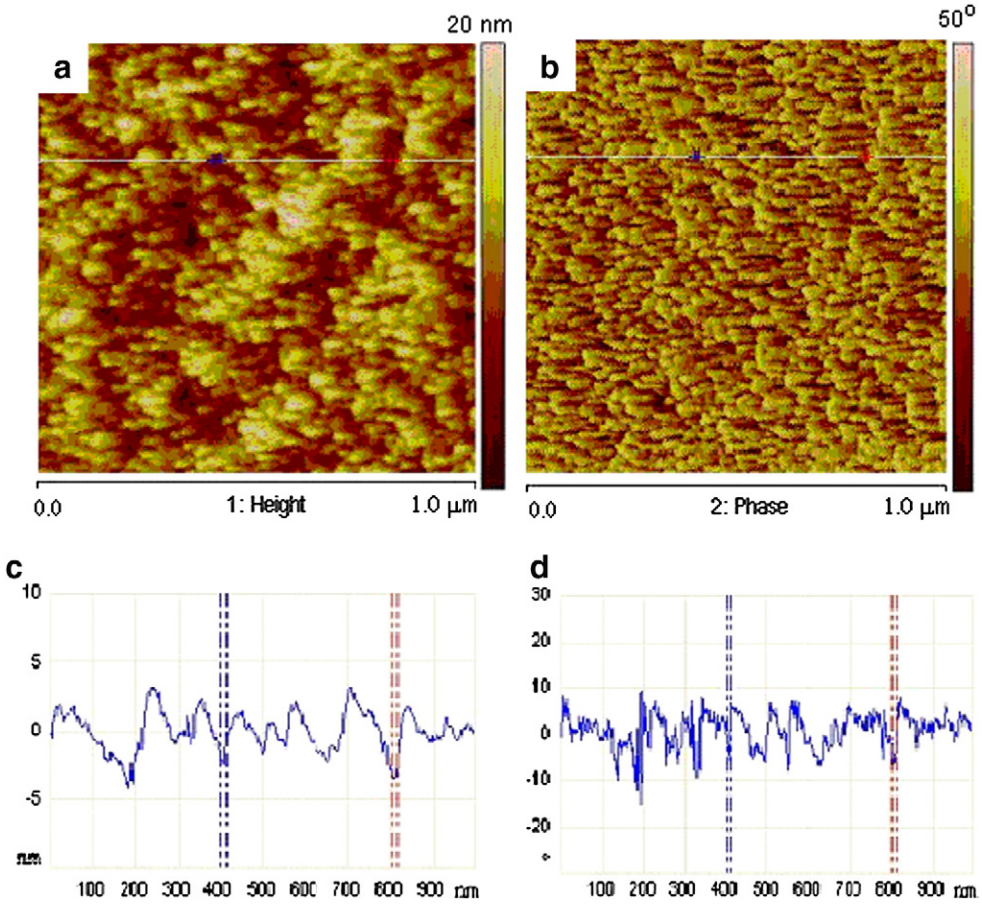

Fig. 8. Determination of the pore size (diameter) of the membrane PA6DT-C from topography and phase images using line profiles. (a) topography, (b) phase image, (c) determination of pore size from 1 µm topography, and (d) determination of pore size from 1 µm phase image.

from different studies is difficult, and strengthens the argument that supporting techniques such as pore size calculation from rejection data should be used in combination with AFM techniques.

Fig. 8 presents the topography and phase image for the PA6DT-C membrane. In membrane studies phase imaging can be used to detect heterogeneous mixing of polymers within a blend membrane; however, there is also the potential to aid in the study of membrane pore structure. The morphology of the polymer membrane in the phase image is much sharper than in the topographical image. Unfortunately, there is no height data available in the phase image as the data is measured as a phase angle. However, X–Y distances can be measured and compared to the same profile from the topographical image. From the topography line profile illustrated in Fig. 8c, the pore radius was determined to be 5.61 nm. Evaluation of the same pore using the phase image (Fig. 8d) gives a pore radius of 4.68 nm. This is arguably due to the fact that as the tapping tip passes over the void of the pore, the interactions between the walls of the pore and the sharp tip are minimum. Thus, AFM phase imaging could provide a more accurate definition and determination of pore size.

Surface roughness was also measured using AFM. At least three AFM images of different parts of the same membrane were analysed and mean values of roughness are reported in Table 3. The general assumption is made that the surfaces of membranes prepared from polymeric materials and used for various membrane separation processes have to be smooth. However, in the process of the preparation of polymeric membranes, the membrane surfaces increase in roughness. The roughness values are different for the basic membrane and modified membranes, varying from 1.39 nm to 2.54 nm for a scanned area of $1 \times 1\ \mu m^2$.

The membrane cross-sectional morphology and internal structure were imaged using SEM and are presented as Fig. 9. Each of the membranes shown has a similar asymmetric structure with a sponge-like top layer and finger-like support structure. The cross-section was imaged at 1000× magnification and the top layer was imaged at 10,000× magnification. The high magnification image of the top layer indicates very little difference, if any, between the two membranes. Therefore, the polyethyleneimine modification layer is thin and certainly less than 15–20 μm which is typical of that for composite membranes. This thin top layer offers little extra hydraulic resistance to flow and explains the significant increase in flux for these membranes when compared to the composite membranes. The resolution of this technique is not sufficient to determine if the modified layer is evenly distributed across the surface or penetrates the pore structure.

4. Conclusions

A review of the fabrication of positively charged NF membranes has been completed. Currently there are a limited number of studies available, thus further research in this area is justified. The preparation of a novel positively charged NF membrane has been demonstrated and will add to the limited number of membranes currently available. This new membrane designated PA6DT-C was fabricated using the phase inversion technique followed by surface modification. The base membrane materials of construction were a

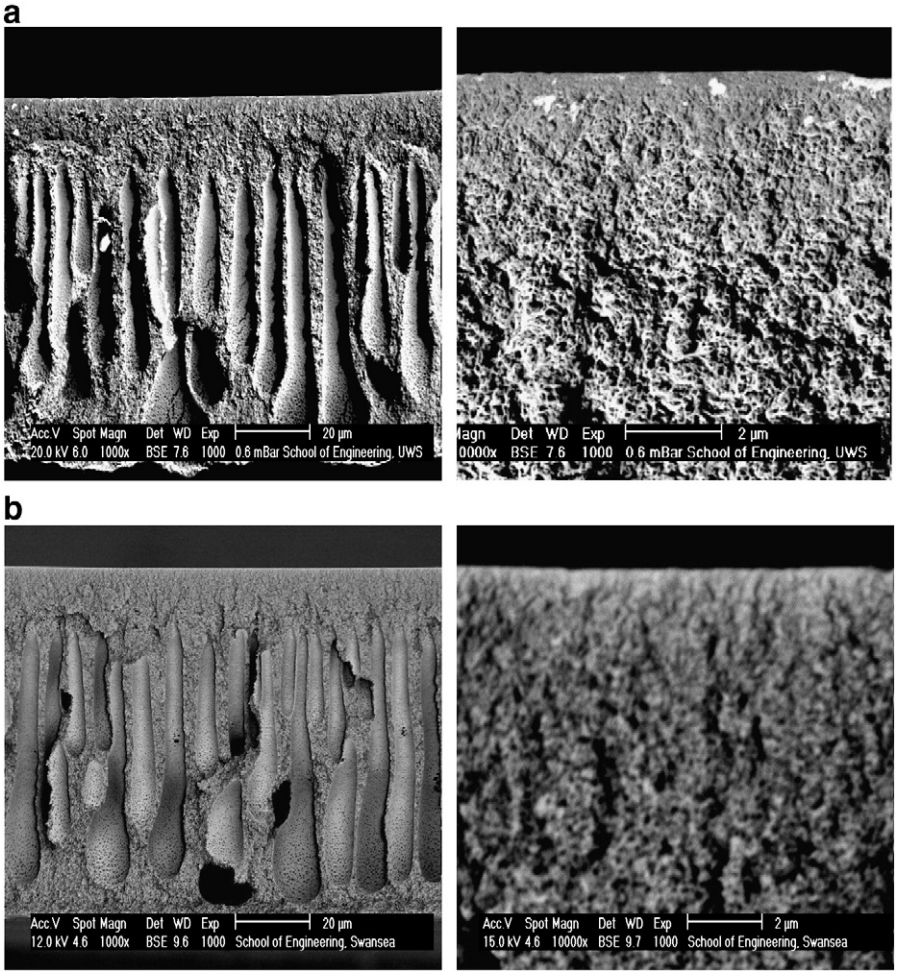

Fig. 9. SEM images of membrane cross-section [left] and top layer [right]. (a) A6DT, and (b) PA6DT-C.

blend of polyetherimide and sulfonated poly(ether ether ketone) modified with polyethyleneimine to achieve the positive charge and cross linked with BUDGE to improve stability. The fabrication process used standard industrial solvents and avoided hazardous materials such as concentrated sulphuric acid, which significantly benefits the scale up potential for a commercial manufacturing process.

The new membrane was characterised using an array of state-of-the-art techniques, including a novel use of AFM. ζ-potential measurements and frontal filtration experimentation demonstrated that the new membrane was indeed positively charged. The effect of pH and salt in the modification solution of polyethyleneimine was also studied. Lowering the pH was found to produce a membrane of larger pore size and lower surface charge, thus lowering rejection and increasing membrane flux. Addition of salt had little effect on the membrane performance characteristics as ionic strength does not significantly affect the adsorption of weak poly-electrolytes on a highly charged surface. The performance characteristics evaluated for this new membrane were very favourable, with a membrane flux of approximately 20 LMH bar^{-1} and a $MgCl_2$ (divalent cation) rejection of 96%. Thus, this new membrane is suitable for applications such as the recovery of valuable cationic macromolecules in the bioprocess and pharmaceutical industries or removal of multi-valent cations such as dyes and heavy metals from effluents in the paper and pulp, textiles, nuclear, and automotive industries.

References

[1] Tsuru T, Takezoe H, Asaeda M. AIChE 1998;44:765.
[2] Childress AE, Elimelech M. J Membr Sci 1996;119:253.
[3] Schaep J, Vandecasteele C. J Membr Sci 2001;118:129.
[4] Du R, Zhao J. J Appl Polym Sci 2004;91:2721.
[5] Du R, Zhao J. J Membr Sci 2004;239:183.
[6] Wang W, Du Q, Li G. Nanoscience 2006;11:38.
[7] Huang R, Chen G, Sun M, Gao C. Desalination 2009;239:38.
[8] Huang R, Chen G, Sun M, Hu Y, Gao C. J Membr Sci 2006;286:237.
[9] Tongwen X, Weihua Y. J Membr Sci 2003;215:25.
[10] Mulder M. Basic principles of membrane technology. London: Kluwer Academic Publishers; 1996.
[11] Tang B, Xu T, Gong M, Yang W. J Membr Sci 2005;248:119.
[12] Tang B, Xu T, Yang W. J Membr Sci 2006;268:123.
[13] Tang B, Xu T, Sun P, Yang W. J Membr Sci 2006;279:192.
[14] Su Y, Jian X, Zhang S, Wang G. J Membr Sci 2004;241:225.
[15] Yan C, Zhang S, Yang D, Jian X. J Appl Polym Sci 2008;107:1809.
[16] Yan C, Zhang S, Liu C, Yang D, Yang F, Jian X. J Appl Polym Sci 2009;113:1389.
[17] Bowen WR, Cheng SY, Doneva TA, Oatley DL. J Membr Sci 2005;250:1.
[18] Kennedy LA, Kopaciewicz W, Regnier FE. J Chrom 1986;359:73.
[19] Oatley DL, Cassey B, Jones P, Bowen WR. Chem Eng Sci 2005;60:1953.
[20] Bowen WR, Welfoot JS. Chem Eng Sci 2002;57:1121.
[21] Bowen WR, Mohammad AW. Desalination 1998;117:257.
[22] Boussu K, Van der Bruggen B, Volodin A, Snauwaert J, Van Haesendonck C, Vandecasteele C. J Colloid Interface Sci 2005;286:632.
[23] Huang HS, Chen CY, Lo SC, Lin CJ, Chen SJ, Lin SJ. Appl Surf Sci 2006;253:2685.
[24] Ghassemi H, McGrath JE, Zawodzinski Jr TA. Polymer 2006;47:4132.
[25] Donnan GF. J Membr Sci 1995;100:45.
[26] Bowen WR, Welfoot JS. Chem Eng Sci 2002;57:1393.
[27] Hilal N, Al-Zoubi H, Darwish NA, Mohammad AW. Desalination 2005;177:187.
[28] Singh S, Khulbe KC, Matsuura T, Ramamurthy P. J Membr Sci 1998;142:111.
[29] Bessieres A, Meireles M, Coratger R, Beauvillain J, Sanchez V. J Membr Sci 1996;109:271.